Journal of Computer Assisted Tomography
26(4):510–514

$H_2{}^{15}0$ Positron Emission Tomography Validation of Semiquantitative Prostate Blood Flow Determined by Double-Echo Dynamic MRI: A Preliminary Study

Satoshi Muramoto, Hidemasa Uematsu, Norihiro Sadato, Tatsuro Tsuchida, Tsuyoshi Matsuda, Hiroto Hatabu, Yoshiharu Yonekura, and Harumi Itoh

Purpose: Information regarding prostate blood flow as determined by positron emission tomography (PET) with $H_2{}^{15}0$ may provide useful information about tumor diagnosis; however, PET requires a cyclotron for the production of an extremely short half-life (2 minutes) tracer. Therefore, the aim of this study was to propose a complementary index for blood flow as determined by MRI to validate the results and compare them with PET, especially for prostate tissue.

Methods: Six consecutive patients with prostate disease were studied. The two semiquantitative indices for tumor blood flow were calculated from the time–concentration curve measured from double-echo MR images. The theory of nondiffusible tracers by means of indicator dilution theory was applied to MR data. The relative regional blood flow (rrBF) was calculated as the ratio of the relative regional blood volume to relative regional mean transit time. Another proposed index was the maximum height of the time–concentration curve. PET studies were also performed, and absolute blood flow values were calculated for each subject. These indices calculated from different modalities were then compared.

Results: A significant correlation was found between the rrBF and the absolute blood flow as determined by PET ($r^2 = 0.69$, $p < 0.005$). A significant correlation was also found between the maximum height of the time–concentration curve and the absolute blood flow ($r^2 = 0.85$, $p < 0.0001$).

Conclusions: The semiquantitative tumor blood flow indices measured with MRI have a good correlation with the corresponding measurements by PET; therefore, these indices may provide useful information about tumor diagnosis in clinical settings.
Index Terms: Prostate—Cancer—Benign prostate hypertrophy—Blood flow—MRI—Double-echo—Positron emission tomography.

Recently, interest in prostate cancer has increased in many countries. Inaba (1) revealed by positron emission tomography (PET) with $H_2{}^{15}0$ that average blood flow in prostate cancer was significantly higher than that of normal prostate tissue and benign prostate hypertrophy. Therefore, it seems important to investigate blood flow in the diagnosis of prostate disease. PET with $H_2{}^{15}0$ has been considered the gold standard for measuring regional blood flow (rBF) (1,2); however, PET requires a cyclotron for the production of an extremely short half-life (2 minutes) tracer. Therefore, blood supply patterns in prostate cancer have been investigated by dynamic MRI (3–5) instead of PET. The usefulness of dynamic MRI for the detection of prostate cancer is limited, however, because early enhancement is occasionally observed in benign prostate hypertrophy, resulting in considerable overlap between prostate cancer and benign prostate hypertrophy. Therefore, a complementary index for tumor blood flow may be useful in the diagnosis of prostate cancer in clinical settings. To our knowledge, tumor blood flow measurement by MRI has not been previously validated or compared with the gold standard method, PET.

From the Department of Radiology, Fukui Medical University (S. Muramoto, H. Uematsu, T. Tsuchida, and H. Itoh), Fukui, Department of Cerebral Research, National Institute for Physiological Sciences (N. Sadato), Aichi, General Electric Yokogawa Medical Systems (T. Matsuda), Tokyo, Biomedical Imaging Research Center, Fukui Medical University (Y. Yonekura), Fukui, Japan; and Department of Radiology, University of Pennsylvania Medical Center (H. Uematsu and H. Hatabu), Philadelphia, PA, U.S.A. Address correspondence and reprint requests to Dr. H. Uematsu, Department of Radiology, University of Pennsylvania Medical Center, 3600 Market Street, Suite 370, Philadelphia, PA 19104–2649, U.S.A. E-mail: uematsu@oasis.rad.upenn.edu

DOI: 10.1097/01.RCT.0000028234.30636.26

The aim of this study was to propose a complementary index for blood flow as determined by MRI to validate the results and compare them with PET, especially for prostate tissue.

THEORY

When the theory of nondiffusible tracers by means of indicator dilution theory (6,7) is applied to the MRI data, the regional mean transit time (rMTT) is expressed by the following (6):

$$rMTT = \frac{rBV}{rBF} = \frac{\int_0^\infty C(t)\,dt}{C_{max}} \quad (1)$$

where rBV is the regional blood volume, rBF is the regional blood flow, C(t) is the idealized bolus, and C_{max} is a maximum height of an idealized bolus C(t). After the intravenous injection of contrast agent, the bolus of contrast material reaches a peak flow over some duration; therefore, the measured tissue concentration-time curve [Cm(t)] is a convolution of the tissue concentration-time response to an idealized bolus C(t) and the arterial input function [AIF(t)]:

$$Cm(t) = C(t) \otimes AIF(t) \quad (2)$$

where $\otimes$ means convolution. To obtain the area-to-height ratio, which is necessary in the first equation, accurate AIF must be obtained (7). The approach without deconvolution analysis has been reported (8); however, deconvolution analysis is usually performed (7). Because accurate AIF is not available in most clinical settings, we assumed C(t) to be proportional to Cm(t). The amplitude, shape, and temporal position of C(t) are different from those of Cm(t); however, we hypothesized that the maximum height of the tissue concentration-time curve (Cm_{max}) could be used as an index of rBF.

The Cm(t) can be estimated by the T2* shortening effect of the intravascular contrast agent ($\Delta R2^*$): $\Delta R2^*(t) \propto Cm(t)$. R2* is calculated as follows (9,10):

$$R2^* = [\ln(S_1/S_2)/(TE_2 - TE_1)] \quad (3)$$

where R2* is the relaxivity rate corresponding to the relaxation time T2* ($R2^* = 1 / T2^*$) and S_1 and S_2 represent the signal of the first TE (TE_1) and the second TE (TE_2), respectively. Consequently, $\Delta R2^*$ is:

$$\Delta R2^* = R2^* - R2^*_0 \quad (4)$$

where $R2^*_0$ is the relaxivity rate before the arrival of the contrast agent. The concentration-time curve ($\Delta R2^*$) was fitted to a gamma-variate function to correct for recirculation (11). The relative regional tumor blood volume (rrBV) represents the area under this fitted concentration-time curve ($\Delta R2^*_f$) using the following equation:

$$rrBV = \int_0^\infty \Delta R2^*_f\,dt \quad (5)$$

Relative regional mean transit time (rrMTT) was calculated as the ratio of the first moment of the $\Delta R2^*_f$ curve to rrBV as follows (12):

$$rrMTT = \frac{\int_0^\infty t \times \Delta R2^*_f\,dt}{\int_0^\infty \Delta R2^*_f\,dt} \quad (6)$$

where t is time. Relative regional blood flow (rrBF) was finally calculated as the ratio of the rrBV to rrMTT as follows:

$$rrBF = \frac{rrBV}{rrMTT} \quad (7)$$

MATERIALS AND METHODS

Six consecutive patients were studied (6 men, age range: 60–85 years). All patients were diagnosed as having prostate cancer with benign prostate hypertrophy. Human studies were performed under the guidelines of our hospital committee on clinical investigations. Written informed consent was obtained from all patients.

MRI

MRI was performed with a 1.5-T clinical MR system (Signa Horizon; General Electric Medical Systems, Milwaukee, WI, U.S.A.). Patients were examined in the supine position with a torso-coil encompassing the pelvis. Axial T1-weighted spin-echo (SE) images (repetition time [TR]/echo time [TE]/number of excitations (NEX): 333/10 milliseconds/2) and T2-weighted fast SE images (TR/TE/NEX: 3500/88 milliseconds/4) were obtained (field of view: 24 × 24 cm; matrix size: 256 × 192–256; slice thickness: 4 mm) before the dynamic study. For the dynamic studies of all patients, we used two echoes with TEs of 7 and 20 milliseconds of a spoiled gradient–recalled acquisition sequence ($TR/TE_1/TE_2$/ flip angle: 33.3/7/20 milliseconds/10°; NEX: 0.75; matrix size: 256 × 128; slice thickness: 7 mm; rectangular field of view: 24 ×16 cm). The dynamic images were obtained from a single section corresponding to the slice appearing to have the most malignant prostate tissue. After five images were acquired, gadopentetate dimeglumine (Gd-DTPA; Magnevist; Nihon Schering, Osaka, Japan) at a dose of 0.1 mmol/kg of body weight was rapidly injected intravenously at a rate of 4 ml/s with an MR-compatible power injector (MRS-50; Nemoto, Tokyo, Japan) followed by a 20-ml saline flush. After the bolus administration of Gd-DTPA, a dynamic series of 60 sets of double-echo images were obtained at 2.47-second intervals. For this sequence, the total acquisition time was approximately 150 seconds. After the dynamic studies,

we also obtained contrast-enhanced T1-weighted SE images.

PET Imaging

$H_2{}^{15}O$ PET studies were performed on a different day for each subject using a high-resolution whole-body PET scanner with an 18-ring detector arrangement (Advance; General Electric Medical Systems). The system permits the simultaneous acquisition of 35 transaxial images with interslice spacing of 4.25 mm, allowing multidirectional reconstruction of the images without loss of resolution. The field of view and pixel size of the reconstructed images were 384 mm and 3 mm, respectively. A 10-minute transmission scan was acquired with a ^{68}germanium/^{68}gallium (Ge/Ga) source for attenuation correction. After the bolus administration of 740 MBq of $H_2{}^{15}O$, emission data were acquired for 210 seconds in 18 frames of 5 seconds and 4 frames of 30 seconds each. Arterial input function was measured using manual arterial blood sampling from a wrist artery. The tissue autoradiographic method proposed by Herscovitch et al. (13) was used for the calculation of the rBF.

Data Analysis

For quantitative analysis of MR images, the regions of interest (ROIs) were placed in the prostate on the spoiled gradient–recalled acquisition images. For quantitative analysis to measure the regional absolute blood flow as determined by PET, similar ROIs were placed in the prostate on the corresponding PET images. All ROIs were placed by one radiologist (S.M.) with knowledge of the final pathologic diagnosis. To minimize the effects of parenchymal hemodynamic heterogeneities in the tumor, the ROIs were set to be as large as possible. Twelve ROIs were placed on different lesions in six subjects (9 ROIs for prostate cancer and 3 ROIs for benign prostate hypertrophy). The pathologic diagnosis was confirmed in all patients after both MRI and PET studies.

We compared the relation between rrBF and absolute blood flow values measured by PET with $H_2{}^{15}0$. Moreover, we compared the maximum height of the $\Delta R2^*_f$ ($\Delta R2^*_f$ max as Cm_{max}), determined by double-echo MRI with the absolute blood flow as determined by PET. The relation between rrBF and absolute blood flow as determined by PET was analyzed by simple regression with the Pearson correlation coefficient. The relation between $\Delta R2^*_f$ max and absolute blood flow as determined by PET was also analyzed by the same method. A probability value less than 0.05 was considered to indicate statistical significance.

RESULTS

In all subjects, the procedures were performed safely and without any complications. The mean blood flow values as determined by PET of the prostate cancer were higher than those of the benign prostate hypertrophy (mean ± SD: 0.55 ± 0.29 ml/min/g [prostate cancer] versus 0.32 ± 0.08 ml/min/g [benign prostate hypertrophy]); however, the difference was not statistically significant ($p = 0.38$, Mann-Whitney *U* test). These results are summarized in Table 1.

Figure 1 depicts a typical time-$\Delta R2^*$ curve fitted with gamma function. A significant correlation was found between the rrBF as determined by MRI and the absolute blood flow as determined by PET (Fig. 2; $r^2 = 0.69$, $p < 0.005$). A significant correlation was also found between the $\Delta R2^*_f$ max as determined by MRI and the absolute blood flow as determined by PET (Fig. 3; $r^2 = 0.85$, $p < 0.0001$).

DISCUSSION

The present study demonstrates a significant correlation between rrBF and absolute blood flow as determined by PET. The rrBF calculated from the indicator dilution theory was found to be useful for determining tumor blood flow as well as for evaluating cerebral hemodynamics (12). Furthermore, the relation between $\Delta R2^*_f$ max and absolute blood flow as determined by PET

TABLE 1. *Summary of 12 ROIs in 6 patients with prostate disease*

ROI/#	Patient #/Age	Diagnosis	ROI size (no. of pixels)	Blood flow by PET (mL/min/g)	ΔR2*f max	rrBF (arbitrary units)
1	**1/85 yrs**	**cancer**	**28**	**0.5**	**22.2**	**14.4**
2	**2/60 yrs**	**cancer**	**25**	**0.99**	**47**	**44.1**
3	**2/60 yrs**	**cancer**	**25**	**0.99**	**39**	**28.8**
4	**2/60 yrs**	**cancer**	**25**	**0.66**	**35**	**29.7**
5	2/60 yrs	BPH	27	0.38	10.8	11.4
6	2/60 yrs	BPH	27	0.36	10.9	11.4
7	**3/81 yrs**	**cancer**	**26**	**0.37**	**16.8**	**17.2**
8	**4/65 yrs**	**cancer**	**72**	**0.28**	**19**	**20.9**
9	**4/65 yrs**	**cancer**	**81**	**0.32**	**22**	**22.4**
10	**5/82 yrs**	**cancer**	**26**	**0.3**	**7.9**	**8.4**
11	5/82 yrs	BPH	25	0.23	8	8.5
12	**6/62 yrs**	**cancer**	**26**	**0.4**	**6.3**	**4.2**

BPH, benign prostate hypertrophy; **bold script,** results of cancer (9 ROIs).

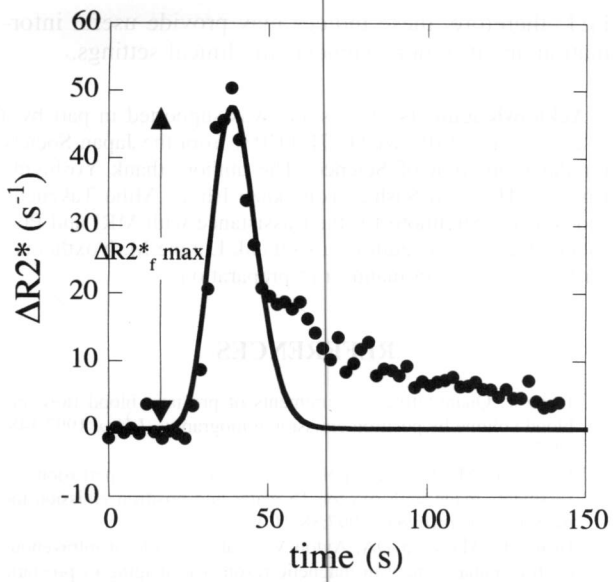

FIG. 1. The representative time course of the ΔR2* values of prostate cancer. The ΔR2* values were plotted by closed circles, and their resulting gamma-fitted curve (ΔR2*$_f$) is represented by a bold line. The maximum height of the ΔR2*$_f$ (ΔR2*$_f$ max) was also compared with the absolute blood flow as determined by positron emission tomography.

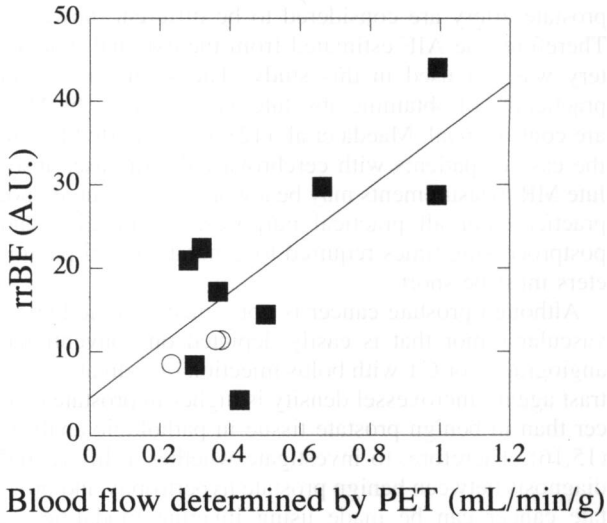

FIG. 2. Plot of the relative regional blood flow (rrBF) versus the absolute blood flow as determined by positron emission tomography (PET). The values of prostate cancer and benign prostate hypertrophy were plotted by solid squares and open circles, respectively. The rrBF is expressed in arbitrary units. The rrBF showed a significant correlation ($r^2 = 0.69$, $p < 0.005$) with absolute blood flow as determined by PET.

showed linear regression. PET is considered the gold standard for measuring rBF (1,2) and was used as a reference method in the current study. In this study, the mean blood flow values in prostate cancer as determined by PET were higher than those in benign prostate hypertrophy. Although the difference was not statistically significant in this study, our purpose was to establish a new diagnostic tool to use instead of PET.

In the theory section, we assumed C(t) to be proportional to Cm(t). The amplitude, shape, and temporal position of C(t) were different from those of Cm(t); however, our hypothesis was also found to apply to the prostate tissues. Furthermore, ΔR2*$_f$ max is much easier to calculate than rrBF, and this simplicity avoids the amplification of noise that can occur with more complex calculations. Therefore, the index (ΔR2*$_f$ max) proposed here may be useful for quickly and inexpensively estimating tumor blood flow semiquantitatively. In a previous publication (14), the maximum signal drop, which corresponds to ΔR2*$_f$ max, was proposed to provide information similar to that about tumor blood volume. Although maximum signal drop may behave similarly to blood volume in tumor cases, we speculate that ΔR2*$_f$ max or maximum signal drop may be a better indicator for tumor blood flow than for tumor blood volume.

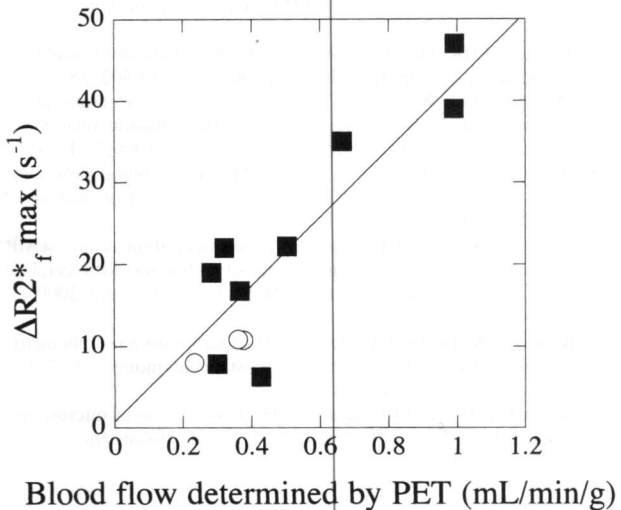

FIG. 3. Plot of ΔR2*$_f$ max versus absolute blood flow as determined by positron emission tomography (PET) with the same format as Figure 2. ΔR2*$_f$ max showed a significant correlation ($r^2 = 0.85$, $p < 0.0001$) with absolute blood flow as determined by PET.

The rrBF and ΔR2*$_f$ max must be considered a semiquantitative evaluation of blood flow, because the AIF was not available and a deconvolution analysis was not applied in the current study. Therefore, we must interpret the data in light of these limitations. In this study, Gd-DTPA at a dose of 0.1 mmol/kg of body weight was rapidly injected intravenously with an MR-compatible power injector, followed by a 20-ml saline flush. The use of the power injector would minimize the variation of the Cm(t). The AIF would have been desirable for this experiment; however, accurate AIF of prostate is not available in the clinical setting. It may be possible to use images of the arteries contained within the field-of-view of the MR images (e.g., external iliac artery) to obtain an estimate of the contrast agent concentration in the blood. The amplitude, shape, and temporal position of the Cm(t) of the external iliac artery and those of the corresponding

prostate artery are considered to be different, however. Therefore, the AIF estimated from the external iliac artery was not used in this study. The significance and practicality of obtaining absolute measurements by MRI are controversial. Maeda et al. (12) have reported that in the case of patients with cerebrovascular disease, absolute MR measurements may be a worthy ideal but are not practical. For all practical purposes, the imaging and postprocessing times required to generate useful parameters must be short.

Although prostate cancer is not a macroscopic hypervascular tumor that is easily depicted on conventional angiography or CT with bolus injection of iodinated contrast agent, microvessel density is higher in prostate cancer than in benign prostate tissue in pathologic analysis (15,16). Therefore, to investigate whether a differential diagnosis between benign prostate hypertrophy and prostate cancer can be made using imaging modalities, a study was conducted in which quantitative measurement of blood flow in prostate lesions was attempted using PET with $H_2{}^{15}0$ (1). In this report (1), the mean blood flow of prostate cancer, benign prostate hypertrophy, and normal prostate tissue were 29.4 ± 7.8 ml/min/100 g, 17.7 ± 5.2 m/min/100 g, and 15.7 ± 7.5 ml/min/100 g, respectively. Blood flow in the prostate cancer was significantly higher than that in the prostate tissue or benign prostate hypertrophy. Therefore, tumor blood flow may be a useful index for differentiating prostate cancer from benign prostate hypertrophy.

Although examining the tumor blood flow by means of indicator dilution theory (6,7) is useful for characterizing the tumor, there is a potential problem with the application of this theory, which was originally introduced as being robust for the study of the normal brain. To use the susceptibility effect of Gd-DTPA for the assessment of tissue blood flow, the measured signal change must be linearly correlated with the local concentration of Gd-DTPA. Tumor vessels are quite different from the normal blood vessels of the brain, however, because they do not express the properties of an intact blood–brain barrier. Hence, after bolus injection, Gd-DTPA causes a T1 shortening effect because of leakage of the contrast medium as well as a T2* shortening effect. Thus, the signal intensity of the tumor derives not only from the vascular spaces but also from the parenchyma itself. We used both the first and second echo images to calculate $\Delta R2^*$ to eliminate this T1 effect. Therefore, in this study, the relation between $\Delta R2^*$ and the local concentration of Gd-DTPA can be assumed to be linear.

In conclusion, we found that the semiquantitative tumor blood flow indices measured with MRI show a good correlation with the corresponding measurements by PET; therefore, these indices may provide useful information about tumor diagnosis in clinical settings.

Acknowledgments: This study was supported in part by a research grant (JSPS-RFTF97L00203) from the Japan Society for the Promotion of Science. The authors thank Yoshiyuki Ishimori, Hiroyuki Sashie, Tomokazu Ishida, Miho Takeuchi, and Katsuya Sugimoto for their assistance with MRI and PET data collection. The authors also thank Lorene M. Yoxtheimer for her assistance in manuscript preparation.

REFERENCES

1. Inaba T. Quantitative measurements of prostatic blood flow and blood volume by positron emission tomography. *J Urol* 1992;148: 1457–60.
2. Bergmann SR. Clinical applications of myocardial perfusion assessments made with oxygen-15 water and positron emission tomography. *Cardiology* 1997;88:71–9.
3. Brown G, Macvicar DA, Ayton V, et al. The role of intravenous contrast enhancement in magnetic resonance imaging of prostatic carcinoma. *Clin Radiol* 1995;50:601–6.
4. Jager GJ, Ruijter ET, van de Kaa CA, et al. Dynamic TurboFLASH subtraction technique for contrast-enhanced MR imaging of the prostate: correlation with histopathologic results. *Radiology* 1997; 203:645–52.
5. Padhani AR, Gapinski CJ, Macvicar DA, et al. Dynamic contrast enhanced MRI of prostate cancer: correlation with morphology and tumour stage, histological grade and PSA. *Clin Radiol* 2000;55: 99–109.
6. Zierler KL. Theoretical basis of indicator-dilution methods for measuring flow and volume. *Circ Res* 1965;16:393–407.
7. Rempp KA, Brix G, Wenz F, et al. Quantification of regional cerebral blood flow and volume with dynamic susceptibility contrast-enhanced MR imaging. *Radiology* 1994;193:637–41.
8. Ishii Y, MacIntyre WJ. Analytical approach to dynamic radioisotope recording. *J Nucl Med* 1971;12:792–9.
9. Uematsu H, Maeda M, Sadato N, et al. Vascular permeability: quantitative measurement with double-echo dynamic MR imaging—theory and clinical application. *Radiology* 2000;214:912–7.
10. Uematsu H, Maeda M, Sadato N, et al. Blood volume of gliomas determined by double-echo dynamic perfusion-weighted MR imaging: a preliminary study. *AJNR Am J Neuroradiol* 2001;22: 1915–9.
11. Thompson HK, Starmer F, Whalen RE, et al. Indicator transit time considered as a gamma variate. *Circ Res* 1964;14:502–15.
12. Maeda M, Yuh WT, Ueda T, et al. Severe occlusive carotid artery disease: hemodynamic assessment by MR perfusion imaging in symptomatic patients. *AJNR Am J Neuroradiol* 1999;20:43–51.
13. Herscovitch P, Markham J, Raichle ME. Brain blood flow measured with intravenous H2(15)O. I. Theory and error analysis. *J Nucl Med* 1983;24:782–9.
14. Cha S, Lu S, Johnson G, et al. Dynamic susceptibility contrast MR imaging: correlation of signal intensity changes with cerebral blood volume measurements. *J Magn Reson Imaging* 2000;11: 114–9.
15. Brawer MK, Bigler SA, Deering RE. Quantitative morphometric analysis of the microcirculation in prostate carcinoma. *J Cell Biochem Suppl* 1992;16H:62–4.
16. Bigler SA, Deering RE, Brawer MK. Comparison of microscopic vascularity in benign and malignant prostate tissue. *Hum Pathol* 1993;24:220–6.